

# Topological phase transitions for any taste in 2D quasiperiodic systems

Tiago S. Gonçalves<sup>1</sup>, Miguel Gonçalves<sup>2</sup>, Pedro Ribeiro<sup>2,3</sup>, Eduardo V. Castro<sup>1,2,3</sup>, Bruno Amorim<sup>11,2,3</sup>

<sup>1</sup>*Centro de Física das Universidades do Minho e Porto,  
Departamento de Física e Astronomia, Faculdade de Ciências,  
Universidade do Porto, 4169-007 Porto, Portugal*

<sup>2</sup>*CeFEMA, Instituto Superior Técnico, Universidade de Lisboa, Av. Rovisco Pais, 1049-001 Lisboa, Portugal*

<sup>3</sup>*Beijing Computational Science Research Center, Beijing 100084, China*

In this paper we explore the effects of quasiperiodicity in paradigmatic models of Chern insulators. We identify a plethora of topological phase transitions and characterize them based on spectral and localization properties, by using a wealth of exact numerical methods. Contrary to uncorrelated disorder, gap closing and reopening topological transitions can be induced by quasiperiodicity. These can separate widely different phases, including (i) trivial and Chern insulators, both with ballistic states near the gap edges; (ii) Chern insulators with critical states around the gap edges or (iii) Chern and trivial insulators respectively with ballistic and localized gap-edge states. Transition (i) is of the same nature as clean-limit topological transitions due to the ballistic character of the gap-edge states, but at the same time resembles (quasi-)disorder driven topological Anderson insulator phenomena. On the other hand, transitions (ii) and (iii) have no clean-limit counterpart. Additionally, quasiperiodicity can also induce topological transitions into a trivial state for which the gap closes and does not reopen, a scenario that resembles more what is observed with uncorrelated disorder. However, we found that such transitions can also be non-conventional in that they can be accompanied by the emergence of intermediate metallic and critical phases where the Chern number is not quantized. Our results show that a rich variety of topological phase transitions, not previously realized experimentally nor predicted theoretically can be attained when applying quasiperiodic modulations to simple models of Chern insulators. Such models have previously been realized experimentally in widely different platforms, including in optical lattices and photonic or acoustic media, where quasiperiodicity effects can be incorporated. The novel topological phase transitions here unveiled can therefore in principle be observed experimentally with state-of-the-art techniques.

## I. INTRODUCTION

Topological insulators are currently a hot topic of research due to their unusual properties when compared to trivial, common band insulators [1–4]. After the discovery of the quantum Hall effect [5] and its theoretical explanation using concepts of topology [6, 7], the quantum anomalous Hall effect, where a topological phase can be induced without the need of an applied homogeneous magnetic field, was proposed by Haldane [8]. This was later realized experimentally on several systems under zero net magnetic field [9–12]. This makes quantum anomalous Hall insulators, or Chern insulators according to the topological classification [4], highly appealing systems to study quantum topological matter at the fundamental level, and to explore possible applications of their distinctive feature – topologically protected gapless surface states.

Topological systems are known to be robust to effects of uncorrelated disorder [13] as long as these do not break any fundamental symmetry. In the case of quantum Hall systems and anomalous quantum Hall insulators, disorder is even crucial for the observation of quantized Hall conductivity, since it localizes every state except for those responsible for the quantized Hall current [14–16]. A well quantized Hall plateau is then the consequence of the Fermi level laying in the gap (filled with localized

states) which separates the extended states that carry the topological invariant. Increasing disorder strength leads, generally, the Chern insulator to a trivial phase [17, 18], under the standard mechanism referred to as “levitation and annihilation” of extended states [16], although exceptions have been identified [19, 20]. Interestingly, topological Anderson insulator phases have also been discovered, in which disorder is responsible to drive a phase transition from trivial to topological phases [21–25].

A different class of systems that break translational invariance, where even more exotic localization properties can occur, are quasiperiodic systems (QPS). These systems have received a lot of attention due to their non-trivial localization properties in one [26–30] and higher [31–39] dimensions. In generic QPS, there can be fully extended, localized and critical phases even in 1D [40–48], while the same is not possible in general in the presence of uncorrelated disorder. More recently, renewed attention has been drawn to QPS in the context of Moiré systems and flatband physics [49, 50], and due to the possibility of being simulated in widely different platforms, including optical lattices [27, 29, 30, 51–57] and photonic [28, 38, 58–62] or even phononic [63–68] media. QPS are also very well-known for their intriguing topological properties [58, 59, 69, 70] that can be seen as originating from a construction using additional (virtual) dimensions [70, 71]

Even though the intrinsic topological properties of QPS have been widely studied, the effects of quasiperiodicity in conventional topological systems, such as Chern insulators, has been less explored [72], with preprints only appearing very recently in this direction [73, 74]. Here, by studying the effect of quasiperiodic potentials on paradigmatic models of Chern insulators, we unveil a myriad of possibilities for the interplay between topology, localization and spectral properties. We obtain the fate of the phase diagrams of the Haldane model and Bernevig-Hughes-Zhang (BHZ) models at half-filling in the presence of quasiperiodic potentials. Additionally, we identify gapped and gapless regions in this new phase diagram and relate all these results with the localization properties of the states at the Fermi level/near the gap edge. We identify a plethora of phase transitions of different nature that were hitherto unknown for two-dimensional systems subject to uncorrelated disorder. Hence, we aim to show that quasi-disorder/quasiperiodicity offers a rich playground to explore new and interesting phenomena in topological systems that are alien to clean systems and systems subjected to random disorder.

In Fig. 1 we provide a summary of the most important results obtained for the Haldane model subject to an incommensurate potential. Naturally, for large strengths of the potential  $V$ , the topological phase of the original system is destroyed. For  $m = 0$  we identify an interesting scenario where the Chern insulator (CI) is first suppressed because the system enters gapless normal (diffusive) and critical metallic phases (respectively NM and CM), in which case the Chern number becomes non-quantized (but finite), before it becomes a gapless Anderson insulator (AI) with null Chern number at larger  $V$  [Fig. 1(b)]. This is corroborated by the energy gap and real-space fractal dimension results in Figs. 1(b,d) respectively. Additionally, we see the emergence of a CI phase with  $C = 1$  starting from a trivial/normal insulator (NI) phase [indicated by the dashed red line in Fig. 1(a)], accompanied by the closing and reopening of the gap [see Fig. 1(c)]. This situation is analogous to the topological Anderson insulator, with the important difference that the gap edge states in both phases are ballistic (characterized by a vanishing momentum-space fractal dimension  $\gamma_k$ ). Such transition is therefore of the same nature as topological transitions in the clean limit, which is not possible under uncorrelated disorder [Fig. 1(c)]. For even higher potential strength, an additional gap closing and reopening transition takes place into a trivial phase with localized gap-edge states (characterized by a vanishing real-space fractal dimension  $\gamma$ ). Adding a quasiperiodic potential to the BHZ model also gives rise to interesting unconventional phase transitions. Examples are shown in Fig. 2, where there is a  $V$ -driven topological phase transition between two gapped [Fig. 2(b)] topological phases with symmetric Chern numbers (CI and CCI). The gap edges within these phases contain critical states around

the transition, that are characterized by non-integer fractal dimensions [see Fig. 2(c)].

The paper is organized as follows: In Sec. II, we introduce the studied models and briefly explain the numerical methods employed throughout the manuscript. In Sec. III we carry out a detailed numerical analysis of the different possible transitions, that includes the characterization of topological, spectral and localization properties. In Sec. IV the key results are summarized their implications are discussed.

## II. MODELS AND METHODS

We start by considering the Haldane model [8] with Hamiltonian written as

$$H_0 = -t \sum_{\langle i,j \rangle} c_i^\dagger c_j + t_2 \sum_{\langle\langle i,j \rangle\rangle} e^{i\phi_{i,j}} c_i^\dagger c_j + \eta \sum_i \zeta_i c_i^\dagger c_i + \text{H.c.}, \quad (1)$$

Here,  $c_i^\dagger (c_i)$  are creation (annihilation) operators defined in the two triangular sub-lattices  $A$  and  $B$  that form the honeycomb lattice. The first term in Eq. (1) corresponds to hopping between nearest neighbor sites  $\langle i, j \rangle$ , and couples sublattices  $A$  and  $B$ . The second term describes complex next-to-nearest neighbor hopping between sites  $\langle\langle i, j \rangle\rangle$ , with amplitude  $t_2 e^{i\phi_{ij}}$  and  $\phi_{ij} = \nu_{ij} \phi$ , where  $\nu_{ij} = (2/\sqrt{3})(\hat{\mathbf{d}}_1 \times \hat{\mathbf{d}}_2) = \pm 1$  with  $\hat{\mathbf{d}}_1$  and  $\hat{\mathbf{d}}_2$  two unit vectors along the two bonds connecting  $\langle\langle i, j \rangle\rangle$ .

In the following  $t$  is set to unity and  $t_2 = 0.2t$  which ensures a direct gap with no band overlapping [8]. The third term corresponds to a staggered potential, where  $\zeta_i = 1$  if  $i \in A$  and  $\zeta_i = -1$  if  $i \in B$ . These last two terms are respectively responsible for breaking time-reversal and inversion symmetries and thus for opening non-trivial and trivial topological gaps at the Dirac points, respectively. In the absence of disorder the phase diagram of the Haldane model in the  $(\eta, \phi)$  parameter space encompasses a trivial phase with vanishing Chern number and two topological non-trivial phases with  $C = \pm 1$  respectively.

We also considered the BHZ, whose Hamiltonian in reciprocal space can be written as

$$H(\vec{\mathbf{k}}) = \vec{\mathbf{h}}(k) \cdot \vec{\sigma}, \quad (2)$$

Where  $\vec{\sigma}$  is the Pauli matrices vector  $\vec{\sigma} = (\sigma_x, \sigma_y, \sigma_z)$  and

$$\vec{\mathbf{h}}(k) = (\sin(k_x), \sin(k_y), M - t\cos(k_x) - t\cos(k_y)).$$

The system is gapped for every value of  $M$  except  $M = \{0, -2, 2\}$ , where the topological phase transitions take place. In what follows, we set  $t = 1$ .

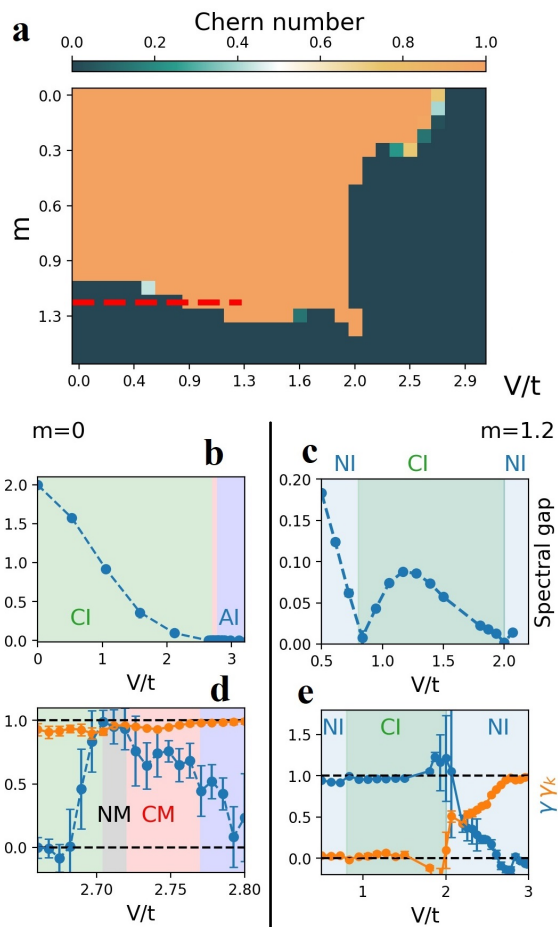


FIG. 1: Summary of results for the Haldane model subjected to a quasiperiodic potential of strength  $V$ , and with  $t_2 = 0.2$  [see Eqs. 1,3]. (a) Phase diagram of the topological phases for a system of size  $N_{\text{u.c.}} = 34 \times 34$  with an average over 50 configurations of random  $\vec{\mathbf{r}}_0$  [Eq. 3] and phase twists. (b,c) Spectral gap for a system of size  $N_{\text{u.c.}} = 144 \times 144$ , respectively for  $m = 0$  and  $m = 1.2$ . We see that in the region where the system is a topological insulator with  $C = 1$  the system has non-zero gap. (d,e) Fractal dimension as a function of quasi-disordered potential for  $m = 0$  and  $m = 1.2$ . The different phases are labelled as Chern insulator (CI), normal metal (NM), critical metal (CM), Anderson insulator (AI) and gapped trivial/normal insulator (NI).

The quasiperiodic potential is introduced in both models through the term

$$V_{\text{qp}}(\vec{\mathbf{r}}) = V \sum_{\vec{\mathbf{b}}_i} \cos\left(\beta(\vec{\mathbf{r}} - \vec{\mathbf{r}}_0) \cdot \vec{\mathbf{b}}_i\right). \quad (3)$$

where  $\beta$  is an irrational number that is responsible for the incommensurate character of this potential,  $\vec{\mathbf{b}}_i$  are the primitive vectors of the reciprocal lattice and  $\vec{\mathbf{r}}_0$  is

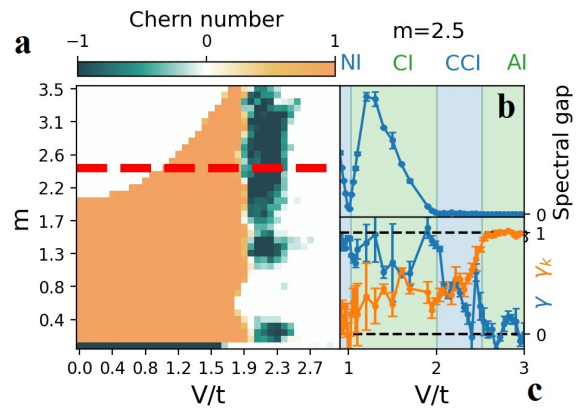


FIG. 2: (a) Phase diagram of the topological phases of the BHZ model with  $m = 2.5$ . These results were obtained for a system of size  $N_{\text{u.c.}} = 34 \times 34$  with an average over 50 configurations. (b) Evolution of the spectral gap as a function of quasi-periodic strength for  $m = 2.5$  [indicated by red dashed line in (a)]. The different phases are labelled as gapped trivial/normal insulator (NI), Chern insulator (CI), critical Chern insulator (CCI) and Anderson insulator (AI). (c) Fractal dimension as a function of quasi-periodic strength.

a shift in the center of the potential. In the case of the quasiperiodic Haldane model we take this quasiperiodic potential to be the same in both sublattices, however, in the case of the BHZ we take this potential to take symmetric value in each sublattice.

In practice, we wish to obtain numerical results for increasingly large unit cells of these quasiperiodic systems, and in order to do this we need  $\beta$  to have a series of rational and commensurate approximants. To meet this condition in the best way possible, we chose  $\beta$  to be the golden ratio,  $\varphi = \frac{1+\sqrt{5}}{2}$ , which can be approximated by the ratio of consecutive members of the Fibonacci sequence,  $f_{n+1}/f_n \rightarrow \varphi$ . Additionally, the numerics are obtained for different configurations of potential center shift  $\vec{\mathbf{r}}_0$  and the twists,  $\theta$ , of the twisted boundary conditions, defined as

$$\begin{aligned} \phi_n^\theta(x + L_x, y) &\equiv \langle x + L_x, y | \phi_n^\theta \rangle = \phi_n^\theta(x, y) e^{i\theta_x} \\ \phi_n^\theta(x, y + L_y) &\equiv \langle L_x, y + L_y | \phi_n^\theta \rangle = \phi_n^\theta(x, y) e^{i\theta_y}. \end{aligned}$$

In the following, we extend the phase diagram of the Haldane model and the model on the square lattice by increasing the quasidisorder strength until the topological phases are destroyed. We identify the topological nature of each phase by computing the Chern number using Fukui's method [75] as implemented in Ref. [76], a variant that is suitable to deal with systems with broken translational invariance.

The localization properties are probed using inverse participation ratios (IPR). To define them, we start

by writing a given eigenstate of the Hamiltonian  $|\phi_n\rangle$  in the local site basis as  $|\phi_n\rangle = \sum_i \phi_{\vec{r}_i}^n |\vec{r}_i\rangle$ , where  $|\vec{r}_i\rangle = c_i^\dagger |0\rangle$ . Then, the real-space IPR is defined as  $\text{IPR}_n = \sum_i |\phi_{\vec{r}_i}^n|^4$ . By carrying out a fourier transform for the real-space amplitudes  $\phi_{\vec{r}_i}^n$ , we get momentum-space amplitudes through which we can compute the momentum-space IPR - the  $\text{IPR}_k$  - in the same way. The finite-size scaling behaviour of these quantities provides a good metric to fully understand the localization properties of a given state. In particular, we can study the *fractal dimension*,  $\gamma$  ( $\gamma_k$ ), defined as

$$\text{IPR} \sim \frac{1}{N_{\text{sites}}^\gamma} \quad \text{IPR}_k \sim \frac{1}{N_{\text{sites}}^{\gamma_k}},$$

where  $N_{\text{sites}}$  is the total number of sites in the system. For ballistic (localized) states we have  $\gamma = 1$ ;  $\gamma_k = 0$  ( $\gamma = 0$ ;  $\gamma_k = 1$ ), while for diffusive (normal) metallic states we have  $\gamma = \gamma_k = 1$ . Finally, for critical states the fractal dimensions take non-integer values either in real or momentum-space, or in both.

Finally, to study spectral properties of our system, namely the spectral energy gap, we used both exact diagonalization or the the Kernel Polynomial Method (KPM) as implemented in the KITE quantum transport software [77].

### III. RESULTS

#### A. Quasiperiodic Haldane model

In this section discuss in detail the results obtained for the Haldane model subject to an incommensurate potential, modeled in the fashion described in the previous section. The topological phase diagram is shown in Figure 1(a). We can see that for small  $V$  the topological phase is robust. However, for sufficiently high quasidisorder there is always a suppression of the topological phase. Another relevant feature is the presence of reentrant behaviour indicated by the dashed red line, where we see an analogous situation to the topological Anderson insulating phenomena observed for uncorrelated disorder in the sense that a topological phase is induced by the presence of quasidisorder.

In the following sections, we will study in detail two cases: the quasi-disorder-driven phase transition (i) from a topological to a trivial phase and (ii) from a trivial gapped phase to a topological quasidisordered insulator and back to trivial insulator.

We describe the phases of our system by taking into account three main characteristics: the spectral energy gap, the topological invariant, and the localization of states near the gap edge. In order to minimize finite-size effects, we extrapolated the spectral gap to the thermodynamic

limit,  $N_{\text{sites}} \rightarrow \infty$ , by making a linear regression of the value of the gap as a function of  $1/N_{\text{sites}}$  and extracting the predicted gap size for  $1/N_{\text{sites}} = 0$ .

#### 1. From a topological to a trivial phase

Figure 3(a) shows a cut of the phase diagram in Fig. 1(a) at  $m = 0$ . Clearly, for low values of quasidisorder we are in the presence of a Chern insulator characterized by  $C = 1$ . We can also see in Figs. 3(b,c,e) that in this region our system is gapped. Additionally, we can characterize the localization properties of the states of the gap edge in this region using the IPR in conjunction with the fractal dimension. These results are shown in Fig. 3(d), indicating localized states, with fractal dimension compatible with 0. For  $V \gtrsim 2.7$ , the system enters a gapless phase, as shown in Fig. 3(e), where the thermodynamic limit extrapolation of the energy gap is compatible with 0. At sufficiently large  $V$ , the system enters a gapless topologically trivial phase with non-quantized Chern number. As shown in Fig. 3(d), this gapless region hosts a small normal (diffusive) metal (NM) region with  $\gamma \approx 1$ , and a critical region (CM) where the fractal dimension exhibits an intermediate value of  $\gamma \approx 0.75$ , robust to increasing the system size (see also some explicit finite-size scalings of the IPR in Fig. 3(f), from which  $\gamma$  was extracted). Note, however, that in this case we only observe real-space fractality since  $\gamma_k \approx 1$  as previously seen in Fig. 1(d). At even larger  $V$ , the system remains gapless, but the Chern number becomes exactly zero, which implies the presence of localized states at the Fermi level. This is further corroborated by the decrease in  $\gamma$  in this regime: we expect  $\gamma \rightarrow 0$  in the thermodynamic limit. Thus, this phase is analogous to an Anderson insulator (AI) observed with uncorrelated disorder, that in this case is instead induced by the presence of quasi-disorder. What is notable about this transition, however, is that it is mediated by a gapless region that hosts diffusive or critical states at the Fermi level. These are evidenced once again in Fig. 3(d) where we see, after a small normal (diffusive) metal region with  $\gamma \approx 1$ , a region where the fractal dimension exhibits an intermediate value of  $\gamma \approx 0.7$ , robust to increasing the system size.

#### 2. From trivial to Chern insulator and back to trivial

We now analyse in detail the situation where we start in a topologically trivial phase and a Chern insulator phase is induced by quasi-disorder. The Chern number calculations are shown in Fig. 4(a). In this case, unlike the one considered in the previous section, our system is gapped for every value of  $V$  except where the topological transitions between the gapped normal insulators (NI) and Chern insulator (CI) happen. This re-

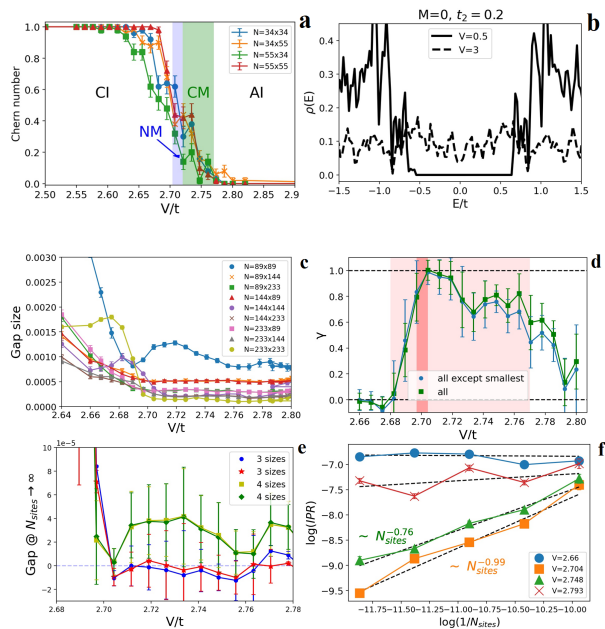


FIG. 3: (a) Chern number as a function of incommensurate potential strength  $V/t$  for various system sizes averaged over 50 configurations. (b) DoS of the Haldane model for  $V = 0.5$  (CI phase) and  $V = 3$  (AI phase) obtained with KPM. (c) Evolution of the spectral gap for different system sizes for the Haldane model with  $m = 0$ . (d) Value of the spectral gap in the limit  $N_{\text{sites}} \rightarrow \infty$  obtain through linear regression. The different curves represent different sets of system sizes used to perform the linear regression. For 3 sizes we used ( $N_{\text{sites}} = 233 \times 233, 144 \times 233, 144 \times 144$  and  $N_{\text{sites}} = 233 \times 233, 233 \times 144, 144 \times 144$ ), and for 4 sizes we used ( $N_{\text{sites}} = 233 \times 233, 144 \times 233, 144 \times 144, 233 \times 89$  and  $N_{\text{sites}} = 233 \times 233, 233 \times 144, 144 \times 144, 89 \times 233$ ). In (f) we explicitly represent a few the finite-size scalings of IPR for a few selected values of quasi-disorder.

sult is clearly evidenced in Fig. 4(b), where we plot the thermodynamic-limit extrapolations of the finite-size gap calculations shown in Figs. 4(c,d).

The IPR and  $\text{IPR}_k$  data used to compute the fractal dimensions in Fig. 1(e) are shown in Fig. 5. There, we see that the  $\text{IPR}_k$  becomes system-size independent in the small- $V$  NI phase and in the CI phase, signaling the presence of ballistic gap-edge states in both. Upon increasing  $V$ , we have a transition into a gapped insulator at  $V = 2.00 \pm 0.07$ . At this large- $V$  NI phase, however, the IPR becomes constant sufficiently away from the transition, signaling the presence of localized gap-edge states. As we decrease  $V$  and approach the transition, the IPR starts to decrease with system size. Nonetheless, we expect the gap-edge states to be localized in the large- $V$  NI phase, but with a localization length that diverges at

the transition - indeed we observe that the IPR, that is inversely proportional to this localization length, sharply increases with  $V$  as we move away from the transition. Since close to the transition the localization length can be very large it is natural that we do not yet see the IPR converging to a constant for the available system sizes, that are smaller than this length. Therefore, in summary we unveiled two types of transitions with the gap closing and reopening mechanism: one in which the gap-edge states are ballistic, which is the same mechanism behind topological transitions in clean systems; and another in which the gap edge states change from ballistic to localized, with no counterpart in the clean limit.

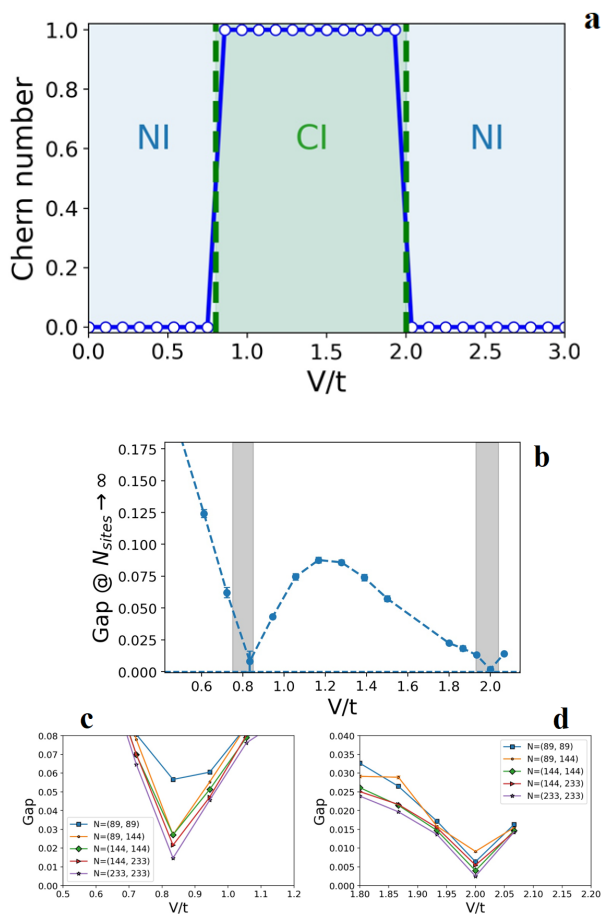


FIG. 4: (a) Chern number results for the Haldane model with a staggered mass  $m = 1.2$ . We identify three distinct phases of our system controlled by the amplitude of the quasi-periodic potential: a normal insulator phase, a Chern insulator phase, and, finally, an Anderson insulator-like phase. These results were obtained for a system with dimensions  $34 \times 34$  averaged over 30 configurations. (b) Gap size in the limit  $N_{\text{sites}} \rightarrow \infty$  obtained through linear regression. The shaded grey areas represent the regions where we expect to find the topological phase transitions. (c) and (d) show a zoom around the first and second gap closing (respectively) with different system sizes represented.

3.

### B. Quasiperiodic BHZ Model

In this section, we study the quasiperiodic BHZ described in II. We have seen the topological phase diagram in Fig. 2(a). Here we analyse the transitions crossed by the dashed red line in this figure in more detail. Con-

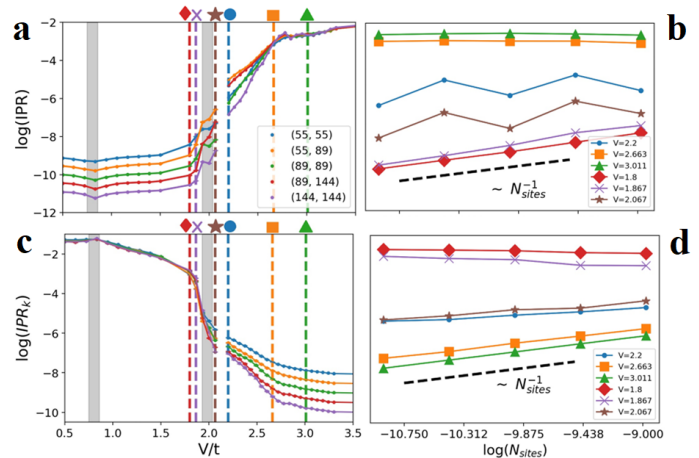


FIG. 5: (a) Value of  $\log(\text{IPR})$  as a function of quasi-periodic strength  $V/t$  for different system sizes. The shaded regions indicate where we saw the topological phase transitions. Once again, the shaded grey areas represent the regions where we expect to find the topological phase transitions in Figure 4(a). (b)  $\log(\text{IPR})$  vs  $1/N_{\text{sites}}$  for a few values of incommensurate potential strength. (c) and (d) show the same as figures (a) and (b) but for the values of the  $\text{IPR}_k$ .

trary to the Haldane model, increasing quasi-disorder at fixed  $m$  can induce two topological phases with distinct Chern numbers and therefore a richer phase diagram.

Setting  $m = 2.5$ , we see that 3 distinct topological transitions occur: (i) from a NI to a CI, (ii) from a CI to a distinct CI, and finally, (iii) from a CI to an AI. Below, we once again characterize these transitions using the same metrics used for the Haldane model. The first transition is qualitatively identical to the transition described in III A 2 for the Haldane model, and thus we will not dwell on it again.

#### 1. Chern Insulator to Critical Chern Insulator

The second transition is from a  $C = -1$  CI to a  $C = 1$  CI as shown in Fig. 6(a). The thermodynamic-limit extrapolation of the gap in Fig. 6(b) suggest that this is a gap closing and reopening transition since the system is gapped in both phases. Even though no conclusive gap closing point is observed across the transition, the change in Chern number requires that this must be the case and we just missed the precise point in the numerical simulations.

For the  $C = -1$  CI, the fractal dimension results in Fig. 2 are not very conclusive and suffer from severe finite-size effects, as evidenced by the very large error bars. The reason for these large errors can be seen in Fig. 7, where no monotonic scaling is observed for the  $\text{IPR}$  and  $\text{IPR}_k$  as a function of system size. Nonetheless,

close to the transition into the  $C = 1$  phase, our results strongly suggest that the gap-edge states are critical. A clear example is shown in detail in Figs. 7(g,h), where we see that the size dependence of the IPR and  $\text{IPR}_k$  data for  $V = 1.6$  is very well described by a power-law with fractal dimensions  $\gamma \approx \gamma_k \approx 0.6$ . At the  $C = 1$  phase, on the other hand, the gap-edge states are clearly critical, being fractal both in real and momentum-space for the whole range of  $V$  within this phase. This is unveiled by the clear scaling of both IPR and  $\text{IPR}_k$  in Fig. 7 yielding the intermediate fractal dimensions shown in Fig. 2. We therefore call this phase the critical Chern insulator (CCI). We therefore have seen that on both sides of the CI-CCI transition, the gap-edge states are critical, which is a novel feature compared to uncorrelated disorder, for which the eigenstates only become critical exactly at the transition. Note that this phase should be distinguished from the CM phase seen in subsection III A 1 for the Haldane model, since in that case we were in the presence of a gapless system and the Chern number was non-quantized. In the CCI, the system is gapped and topological, but the gap-edge states are critical.

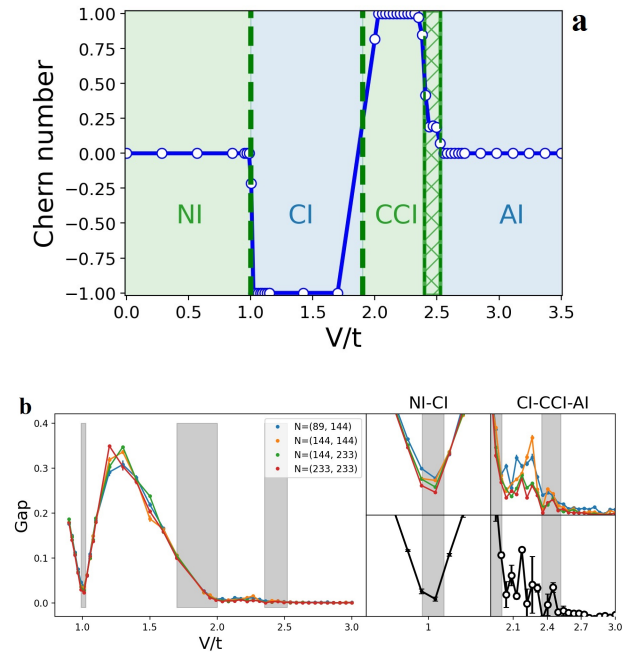


FIG. 6: (a) Topological invariant as a function of quasi-periodic potential strength. We observe three topological transitions at  $V = (1.007 \pm 0.017) t$ ,  $V = (1.95 \pm 0.15) t$ , and  $V = (2.435 \pm 0.170) t$ . The criss-crossed green region denotes a range of value of  $V/t$  where our results are not yet conclusive, and is discussed in more detail in the body of the text. These results are obtained for a system with size  $N_{\text{sites}} = 34 \times 34$  averaged over 200 configurations. (b) Evolution of the spectral gap as a function of quasi-periodic disorder strength for different system sizes. In the insets we show the two regions of interest with the panels on top representing the values of the spectral for different system sizes and the figures below showing the value in the limit  $N_{\text{sites}} \rightarrow \infty$  obtain through linear regression.

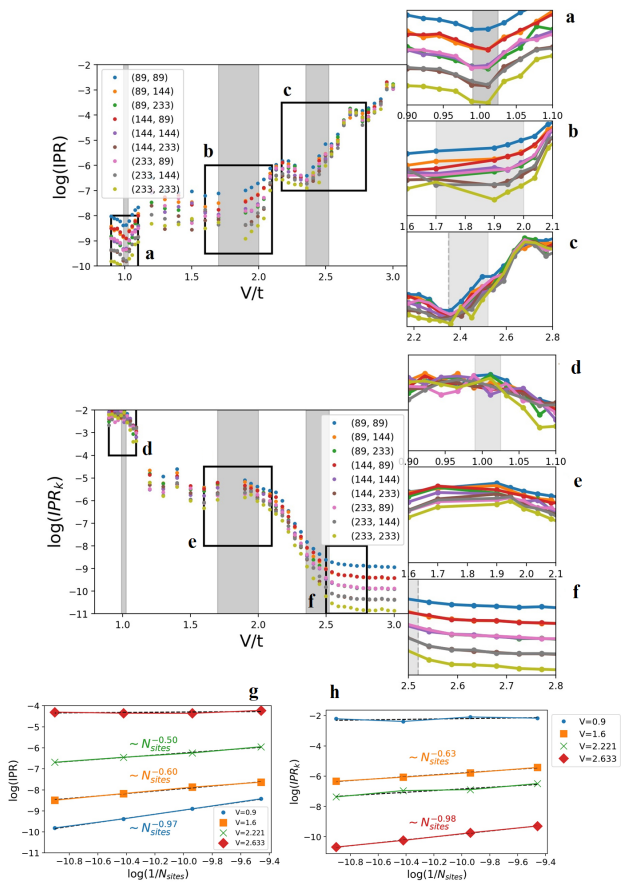


FIG. 7: (a), (b), and (c) [(d), (e) and (f)] show the value of  $\log(\text{IPR})$  [ $\log(\text{IPR}_k)$ ] as a function of quasi-disorder strength for different system sizes. In the inset axes are magnified areas of interest to our study of the localization properties close to the topological phase transitions (represented by the shaded regions). (g,h) Scaling of the IPR and  $\text{IPR}_k$  for a few selected values of quasi-disorder.

## 2. Critical Chern Insulator - Anderson Insulator

Increasing the incommensurate potential even further has evident effects both in the spectral gap and in the localization of states. We can see in Figure 6(b) that the data for the spectral gap is very noisy presenting big fluctuations for all sizes, which manifests itself in the big error bars in the values obtained through thermodynamic-limit extrapolation of the gap. Nevertheless, we are fairly certain that before the last topological phase transition, still in the CCI phase, we have a, albeit very small, non-vanishing spectral gap. The reason being that, since in that region we have, undoubtedly, quantized Chern number, and the localization data in Figs. 2(c), 7 indicates that the eigenstates are critical around the gap edge, the

only way to conciliate these two facts is to have finite spectral gap.

The mechanism for the last topological phase transition, that happens around the rightmost shaded area in Figs. 6, 7, is however less clear. We see in Fig. 6(b) that the gap seemingly closes at the onset of this region and sharply reopens before closing again. In this latter regime, the system clearly becomes an AI: the eigenstates are localized due to the null value of the Chern number and the convergence of the IPR into a constant shown in Fig. 7(c), which implies that  $\gamma \approx 0$  and  $\gamma_k \approx 1$ , as shown in Fig. 2(c).

## IV. CONCLUSIONS

In this paper, we explored the effects of quasi-disorder on Chern insulators and found that it can lead to a rich and diverse landscape of phase transitions. These go from transitions of the same nature as the conventional transitions in clean systems to transitions with no counterpart both in the clean and randomly disordered cases.

Contrary to uncorrelated disorder, quasiperiodicity can induce gap closing and reopening topological transitions. These can be of widely different nature, including (i) trivial to Chern insulators, both with ballistic states near the gap edges; (ii) Chern to Chern insulators with critical states around the gap edges or (iii) Chern to trivial insulators accompanied by a ballistic-to-localized transition for the gap-edge states. While transition (i) has the same nature of clean-limit topological transitions, transitions (ii) and (iii) have no clean-limit counterpart. Additionally, we can have topological transitions for which the gap closes and does not reopen. Among these, we found an interesting transition from a Chern insulator to a trivial gapless Anderson insulator, with intermediate metallic and critical phases where the Chern number is not quantized. Curiously, we have not found an instance of a gapless topological insulating phase (with localized states at the Fermi level), which is common in systems with random disorder.

Our findings demonstrate that quasi-disorder can induce a greater variety of phase transitions than previously thought - much greater than uncorrelated disorder - and that these transitions can be classified into different categories based on their underlying physical mechanisms. Our results significantly expand the knowledge of the interplay between quasiperiodicity effects and topology in Chern insulators, unveiling a myriad of different phases and phase transitions in simple models that can be experimentally realized in optical lattices [10, 78], photonic [79–81] and acoustic [82, 83] media, and possibly even moiré systems [84].



- 
- [1] M. Z. Hasan and C. L. Kane, *Rev. Mod. Phys.* **82**, 3045 (2010).
- [2] X.-L. Qi and S.-C. Zhang, *Rev. Mod. Phys.* **83**, 1057 (2011).
- [3] B. A. B. with Taylor L. Hughes, *Topological Insulators and Topological Superconductors* (Princeton University Press, 2013).
- [4] C.-K. Chiu, J. C. Y. Teo, A. P. Schnyder, and S. Ryu, *Rev. Mod. Phys.* **88**, 035005 (2016).
- [5] K. V. Klitzing, G. Dorda, and M. Pepper, *Physical Review Letters* **45**, 494 (1980).
- [6] D. J. Thouless, M. Kohmoto, M. P. Nightingale, M. D. Nijs, and M. den Nijs, *Phys. Rev. Lett.* **49**, 405 (1982).
- [7] Q. Niu, D. J. Thouless, and Y.-S. Wu, *Phys. Rev. B* **31**, 3372 (1985).
- [8] F. D. M. Haldane, *Phys. Rev. Lett.* **61**, 2015 (1988).
- [9] C.-Z. Chang, J. Zhang, X. Feng, J. Shen, Z. Zhang, M. Guo, K. Li, Y. Ou, P. Wei, L.-L. Wang, Z.-Q. Ji, Y. Feng, S. Ji, X. Chen, J. Jia, X. Dai, Z. Fang, S.-C. Zhang, K. He, Y. Wang, L. Lu, X.-C. Ma, and Q.-K. Xue, *Science* **340**, 167 (2013).
- [10] G. Jotzu, M. Messer, R. Desbuquois, M. Lebrat, T. Uehlinger, D. Greif, and T. Esslinger, *Nature* **515**, 237 (2014).
- [11] J. G. Checkelsky, R. Yoshimi, A. Tsukazaki, K. S. Takahashi, Y. Kozuka, J. Falson, M. Kawasaki, and Y. Tokura, *Nature Physics* **10**, 731 (2014).
- [12] C. Z. Chang, W. Zhao, D. Y. Kim, H. Zhang, B. A. Assaf, D. Heiman, S. C. Zhang, C. Liu, M. H. Chan, and J. S. Moodera, *Nature Materials* **14**, 473 (2015).
- [13] D. Xiao, M. C. Chang, and Q. Niu, *Reviews of Modern Physics* **82**, 1959 (2010).
- [14] B. Kramer and A. MacKinnon, *Rep. Prog. Phys.* **56**, 1469 (1993).
- [15] M. Onoda and N. Nagaosa, *Phys. Rev. Lett.* **90**, 206601 (2003).
- [16] M. Onoda, Y. Avishai, and N. Nagaosa, *Phys. Rev. Lett.* **98**, 76802 (2007).
- [17] E. Prodan, T. L. Hughes, and B. A. Bernevig, *Phys. Rev. Lett.* **105**, 115501 (2010).
- [18] E. Prodan, *Journal of Physics A: Mathematical and Theoretical* **44**, 113001 (2011).
- [19] E. V. Castro, M. P. López-Sancho, and M. A. Vozmediano, *Physical Review B - Condensed Matter and Materials Physics* **92** (2015), 10.1103/PhysRevB.92.085410.
- [20] E. V. Castro, R. De Gail, M. P. López-Sancho, and M. A. Vozmediano, *Physical Review B* **93**, 245414 (2016).
- [21] J. Li, R.-L. Chu, J. K. Jain, and S.-Q. Shen, *Phys. Rev. Lett.* **102**, 136806 (2009).
- [22] C. W. Groth, M. Wimmer, A. R. Akhmerov, J. Tworzydło, and C. W. Beenakker, *Physical Review Letters* **103** (2009), 10.1103/PhysRevLett.103.196805.
- [23] J. Song, H. Liu, H. Jiang, Q. F. Sun, and X. C. Xie, *Physical Review B - Condensed Matter and Materials Physics* **85** (2012), 10.1103/PhysRevB.85.195125.
- [24] J. H. García, L. Covaci, and T. G. Rappoport, *Physical Review Letters* **114**, 1 (2015).
- [25] C. P. Orth, T. Sekera, C. Bruder, and T. L. Schmidt, *Scientific Reports* **6** (2016), 10.1038/srep24007.
- [26] S. Aubry and G. André, *Proceedings, VIII International Colloquium on Group-Theoretical Methods in Physics* **3** (1980).
- [27] G. Roati, C. D’Errico, L. Fallani, M. Fattori, C. Fort, M. Zaccanti, G. Modugno, M. Modugno, and M. Inguscio, *Nature* **453**, 895 (2008), arXiv:0804.2609.
- [28] Y. Lahini, R. Pugatch, F. Pozzi, M. Sorel, R. Morandotti, N. Davidson, and Y. Silberberg, *Phys. Rev. Lett.* **103**, 013901 (2009).
- [29] M. Schreiber, S. S. Hodgman, P. Bordia, H. P. Lüschen, M. H. Fischer, R. Vosk, E. Altman, U. Schneider, and I. Bloch, *Science* **349**, 842 (2015), arXiv:1501.05661.
- [30] H. P. Lüschen, S. Scherg, T. Kohlert, M. Schreiber, P. Bordia, X. Li, S. Das Sarma, and I. Bloch, *Phys. Rev. Lett.* **120**, 160404 (2018).
- [31] C. Huang, F. Ye, X. Chen, Y. V. Kartashov, V. V. Konotop, and L. Torner, *Scientific Reports* **6**, 32546 (2016).
- [32] J. H. Pixley, J. H. Wilson, D. A. Huse, and S. Gopalakrishnan, *Phys. Rev. Lett.* **120**, 207604 (2018).
- [33] M. J. Park, H. S. Kim, and S. Lee, *Phys. Rev. B* **99**, 245401 (2019), arXiv:1812.09170.
- [34] P. Bordia, H. Lüschen, S. Scherg, S. Gopalakrishnan, M. Knap, U. Schneider, and I. Bloch, *Phys. Rev. X* **7**, 041047 (2017).
- [35] B. Huang and W. V. Liu, *Phys. Rev. B* **100**, 144202 (2019).
- [36] Y. Fu, E. J. König, J. H. Wilson, Y.-Z. Chou, and J. H. Pixley, *npj Quantum Materials* **5**, 71 (2020).
- [37] Y.-Z. Chou, Y. Fu, J. H. Wilson, E. J. König, and J. H. Pixley, *Phys. Rev. B* **101**, 235121 (2020).
- [38] P. Wang, Y. Zheng, X. Chen, C. Huang, Y. V. Kartashov, L. Torner, V. V. Konotop, and F. Ye, *Nature* **577**, 42 (2020).
- [39] M. Gonçalves, H. Z. Olyaei, B. Amorim, R. Mondaini, P. Ribeiro, and E. V. Castro, *2D Materials* **9**, 011001 (2021).
- [40] M. Johansson and R. Riklund, *Phys. Rev. B* **43**, 13468 (1991).
- [41] J. Biddle and S. Das Sarma, *Phys. Rev. Lett.* **104**, 70601 (2010).
- [42] J. D. Bodyfelt, D. Leykam, C. Danieli, X. Yu, and S. Flach, *Phys. Rev. Lett.* **113**, 236403 (2014).
- [43] F. Liu, S. Ghosh, and Y. D. Chong, *Phys. Rev. B - Condens. Matter Mater. Phys.* **91**, 014108 (2015).
- [44] C. Danieli, J. D. Bodyfelt, and S. Flach, *Phys. Rev. B* **91**, 235134 (2015).
- [45] S. Ganeshan, J. H. Pixley, and S. Das Sarma, *Phys. Rev. Lett.* **114**, 146601 (2015).
- [46] T. Liu, X. Xia, S. Longhi, and L. Sanchez-Palencia, *SciPost Phys.* **12**, 27 (2022).
- [47] M. Gonçalves, B. Amorim, E. V. Castro, and P. Ribeiro, (2022), 10.48550/arxiv.2206.13549, arXiv:2206.13549.
- [48] M. Gonçalves, B. Amorim, E. V. Castro, and P. Ribeiro, “Critical phase in a class of 1d quasiperiodic models with exact phase diagram and generalized dualities,” (2022).
- [49] L. Balents, C. R. Dean, D. K. Efetov, and A. F. Young, *Nat. Phys.* **16**, 725 (2020).
- [50] E. Y. Andrei and A. H. MacDonald, *Nature Materials* **19**, 1265 (2020).
- [51] D. J. Boers, B. Goedeke, D. Hinrichs, and M. Holthaus, *Phys. Rev. A* **75**, 63404 (2007).
- [52] M. Modugno, *New Journal of Physics* **11**, 33023 (2009).
- [53] H. Yao, H. Khoudli, L. Bresque, and L. Sanchez-Palencia, *Phys. Rev. Lett.* **123**, 070405 (2019).
- [54] H. Yao, T. Giamarchi, and L. Sanchez-Palencia, *Phys. Rev. Lett.* **125**, 060401 (2020).

- [55] R. Gautier, H. Yao, and L. Sanchez-Palencia, *Phys. Rev. Lett.* **126**, 110401 (2021).
- [56] F. A. An, K. Padavić, E. J. Meier, S. Hegde, S. Ganeshan, J. H. Pixley, S. Vishveshwara, and B. Gadway, *Phys. Rev. Lett.* **126**, 040603 (2021).
- [57] T. Kohlert, S. Scherg, X. Li, H. P. Lüschen, S. Das Sarma, I. Bloch, and M. Aidelsburger, *Phys. Rev. Lett.* **122**, 170403 (2019).
- [58] Y. E. Kraus and O. Zilberberg, *Phys. Rev. Lett.* **109**, 116404 (2012).
- [59] M. Verbin, O. Zilberberg, Y. E. Kraus, Y. Lahini, and Y. Silberberg, *Phys. Rev. Lett.* **110**, 076403 (2013).
- [60] M. Verbin, O. Zilberberg, Y. Lahini, Y. E. Kraus, and Y. Silberberg, *Phys. Rev. B* **91**, 64201 (2015).
- [61] A. D. Sinelnik, I. I. Shishkin, X. Yu, K. B. Samusev, P. A. Belov, M. F. Limonov, P. Ginzburg, and M. V. Rybin, *Advanced Optical Materials* **8**, 2001170 (2020), <https://onlinelibrary.wiley.com/doi/pdf/10.1002/adom.2001170>.
- [62] P. Wang, Q. Fu, R. Peng, Y. V. Kartashov, L. Torner, V. V. Konotop, and F. Ye, *Nature Communications* **13**, 6738 (2022).
- [63] D. J. Apigo, W. Cheng, K. F. Dobiszewski, E. Prodan, and C. Prodan, *Phys. Rev. Lett.* **122**, 095501 (2019).
- [64] X. Ni, K. Chen, M. Weiner, D. J. Apigo, C. Prodan, A. Alù, E. Prodan, and A. B. Khanikaev, *Communications Physics* **2**, 55 (2019).
- [65] W. Cheng, E. Prodan, and C. Prodan, *Phys. Rev. Lett.* **125**, 224301 (2020).
- [66] Y. Xia, A. Erturk, and M. Ruzzene, *Phys. Rev. Applied* **13**, 014023 (2020).
- [67] Z.-G. Chen, W. Zhu, Y. Tan, L. Wang, and G. Ma, *Phys. Rev. X* **11**, 011016 (2021).
- [68] M. Gei, Z. Chen, F. Bosi, and L. Morini, *Applied Physics Letters* **116**, 241903 (2020), <https://doi.org/10.1063/5.0013528>.
- [69] Y. E. Kraus and O. Zilberberg, *Phys. Rev. Lett.* **109**, 116404 (2012).
- [70] O. Zilberberg, *Opt. Mater. Express* **11**, 1143 (2021).
- [71] W. Steurer, *Acta Crystallographica Section A* **53** (1997), 10.1107/S0108767397099868.
- [72] Y. Fu, J. H. Wilson, and J. H. Pixley, *Physical Review B* **104** (2021), 10.1103/physrevb.104.1041106.
- [73] M. F. Madeira and P. D. Sacramento, “Quasidisorder induced topology,” (2022).
- [74] S. Cheng, R. Asgari, and G. Xianlong, “From topological phase to anderson localization in a two-dimensional quasiperiodic system,” (2022).
- [75] T. Fukui, Y. Hatsugai, and H. Suzuki, *Journal of the Physical Society of Japan* **74**, 1674 (2005), <https://doi.org/10.1143/JPSJ.74.1674>.
- [76] Y.-F. Zhang, Y.-Y. Yang, Y. Ju, L. Sheng, R. Shen, D.-N. Sheng, and D.-Y. Xing, *Chinese Physics B* **22**, 117312 (2013).
- [77] S. M. João, M. Anđelković, L. Covaci, T. G. Rappoport, J. M. V. P. Lopes, and A. Ferreira, *Royal Society Open Science* **7** (2020).
- [78] W. Liu, Z. Lin, Z. D. Wang, and Y. Chen, *Scientific Reports* **8**, 12898 (2018).
- [79] Z. Wang, Y. D. Chong, J. D. Joannopoulos, and M. Soljačić, *Phys. Rev. Lett.* **100**, 013905 (2008).
- [80] Z. Wang, Y. Chong, J. D. Joannopoulos, and M. Soljačić, *Nature* **461**, 772 (2009).
- [81] S. Lannebère and M. G. Silveirinha, *Nanophotonics* **8**, 1387 (2019).
- [82] Y. Ding, Y. Peng, Y. Zhu, X. Fan, J. Yang, B. Liang, X. Zhu, X. Wan, and J. Cheng, *Phys. Rev. Lett.* **122**, 014302 (2019).
- [83] G. Ma, M. Xiao, and C. T. Chan, *Nature Reviews Physics* **1**, 281 (2019).
- [84] W. Zhao, K. Kang, L. Li, C. Tschirhart, E. Redekop, K. Watanabe, T. Taniguchi, A. Young, J. Shan, and K. F. Mak, “Realization of the haldane chern insulator in a moiré lattice,” (2022).